Int. J. Heat Mass Transfer. Vol. 33, No. 6, pp. 1281–1288, 1990
Printed in Great Britain

0017-9310/90 $3.00 + 0.00

Heat and mass transfer in metal hydride beds for heat pump applications

H. CHOI and A. F. MILLS
School of Engineering and Applied Science, University of California, Los Angeles, CA 90024-1429, U.S.A.

(*Received* 7 *April* 1989 *and in final form* 18 *September* 1989)

Abstract—Heat and mass transfer in a metal hydride bed is modeled. The model includes heat conduction, hydrogen flow governed by Darcy's law modified for the transitional flow regime, and sorption kinetics assuming that diffusion across the hydride is the rate limiting step. The model parameters are established for $LaNi_{4.7}Al_{0.3}$ alloy using available experimental data. Parametric calculations for a space vehicle heat pump application show the competing effects of heat transfer, hydrogen flow and sorption kinetics limitations. The effect of augmenting heat conduction is demonstrated. Optimum bed thicknesses appear to be in the range 10–20 mm for a 3 min absorption time and $k_b = 1.3 \sim 5$ W m^{-1} K^{-1}.

1. INTRODUCTION

METAL hydrides have considerable potential for sorption heat pumps [1, 2], chemical compressors [3, 4] and for hydrogen storage [5]. Of particular current interest are metal hydride based sorption heat pumps. Sorption heat pumps have many advantages over mechanical heat pumps: they have no wear dependent moving parts, generate negligible mechanical vibration and electromagnetic interference, are relatively simple, and can be powered by waste heat instead of electricity. Metal hydrides are particularly suitable for this purpose: they have fast kinetics and can absorb, and reversibly desorb, large amounts of hydrogen at constant temperature over a pressure plateau where the pressure remains constant while the hydrogen/metal ratio varies. The major difficulties associated with the use of metal hydrides are the hydrogen content capacity limitation, which is less than 2% by weight, a low thermal conductivity, and inadequate reaction kinetic data for many candidate hydrides.

A typical heat pump design for commercial application is the unit reported by Yanoma *et al.* [6]. The unit is essentially a shell and finned tube type heat exchanger, with copper fins to enhance heat transfer through the metal hydride powder. A pair of metal hydrides are contained in one shell separated by a centerplate, with holes for hydrogen flow, filters and thermal insulation. Test data are reported for a large unit, which produces 80°C hot water from 65°C warm water and 15°C cooling water, with 174 kW heat output. The optimum cycle time was found to be about 10 min. The key design problem is to minimize the cycle time, and so reduce the size and weight of the hydride beds. In the case of waste heat recovery in industrial operations, the cost of the metal hydride is a major concern, while for waste heat upgrading on satellites the weight of the metal hydride is critical to the feasibility of the heat pump.

The first step in the design of a hydride heat pump is the selection of a suitable pair or metal hydrides. Numerous metal alloys have been investigated for heat pump application. The necessary thermodynamic properties have been tabulated by Dantzer and Orgaz [7] for 27 candidate alloys. These data allow the determination of the maximum operating temperature range for a given pair of alloys, and for a chosen temperature range, a thermal balance yields the coefficient of performance of the cycle. Specification of the cycle then allows the hydride bed weight to be determined. The next step is to choose a bed configuration and to determine an effective bed thickness which will minimize the cycle time. Previous work, e.g. ref. [8] has shown that heat transfer to/from the bed, and hydrogen flow in/out of the bed are probably the rate limiting processes, because of the fast kinetics, low hydride thermal conductivity, and small hydride particle size (order of micrometers). Thus a heat transfer, mass transfer and fluid flow analysis is required.

Several attempts have been made to analyze hydride bed behavior, but in most of this work the importance of hydrogen flow limitations and the resulting pressure distribution through the bed, has not been recognized. The hydrogen flow limitation is particularly important at low pressures. The finite rate kinetics of the sorption process is expected to be the limiting factor at much shorter cycle times than usually feasible due to the heat transfer and hydrogen flow limitations. Relevant prior analytical work is sparse. Yanoma *et al.* [6] assumed a lumped thermal capacitance model for heat transfer. Such a model is fundamentally incorrect for a conduction limited process (large Biot number) and gives results which scale with bed thickness, rather than bed thickness squared. Mayer *et al.* [9] modeled the behavior of coupled reaction beds properly accounting for heat conduction, but assumed a constant pressure in each bed.

This paper reports the development and use of a model for one-dimensional metal hydride beds which

NOMENCLATURE

c_b	specific heat of hydride bed
c_{pg}	constant pressure specific heat of hydrogen
D	diffusion coefficient, $D_0 \exp(-E_a/\mathscr{R}T)$
D_0	diffusion constant
D^*	diffusion parameter, $4\pi r_o D_0 n_0$
d_p	average particle diameter
E_a	activation energy for hydrogen diffusion through hydride phase
ΔH	heat of formation of hydride
k_b	effective thermal conductivity of the bed
K_D	Darcy permeability
K_{eff}	effective Darcy permeability
Kn	Knudsen number
L	bed thickness
L_c	characteristic length
M	molecular weight
$\dot{m}_H$	mass diffusion rate of hydrogen
n_0	number of hydride particles per unit volume
P	hydrogen pressure
P_{eq}	equilibrium pressure
$\dot{r}$	reaction rate
$\mathscr{R}$	universal gas constant
r_c	radius of hydride front
r_o	outer radius of hydride particle
T	temperature
t	time
u	superficial velocity of hydrogen
z	axial coordinate.

Greek symbols

β	plateau hysteresis factor
ε_b	packed bed void fraction
θ	dimensionless temperature
λ	mean free path
μ	viscosity
ξ	constant defined in equation (3)
ρ	density
ϕ	plateau flatness factor
ω	hydrogen concentration ratio.

Subscripts

0	initial value
b	bed; bulk
eq	equilibrium state
g	hydrogen
i	i-surface, in hydride phase adjacent to alloy
s	s-surface, in gas phase adjacent to hydride phase
u	u-surface, in hydride phase adjacent to gas phase.

accounts for heat conduction, hydrogen flow and reaction kinetics. The governing differential equations are solved numerically. The effect of the key design parameters, bed thickness, and the bed thermal conductivity are explored for a chosen alloy, to show the competing effects of heat transfer and hydrogen flow. The work should be viewed as a precursor to the prediction of the dynamic response of two coupled hydride beds in a heat pump. In addition the model and associated computer code should find application for the evaluation of experiments used to determine hydride reaction kinetics, since one-dimensional beds are usually used for this purpose [8, 9].

2. ANALYSIS

Figure 1 shows an element of a bed comprising of a layer of hydride particles of thickness L. One-dimensional quasi-steady flow of hydrogen is assumed. The mass conservation equation is

$$\frac{d}{dz}(\rho_g u) = -\dot{r}(z, t) \tag{1}$$

where $\dot{r}$ [kg m^{-3} s^{-1}] is the volumetric rate of hydrogen absorption. Darcy's law is used to relate pressure gradient to flow velocity in the particle bed

$$\frac{dP}{dz} = -\frac{\mu u}{K_{eff}} \tag{2}$$

where

$$K_{eff} = K_D[1 + \xi\, Kn]. \tag{3}$$

Here K_D is the conventional Darcy permeability, Kn the Knudsen number and ξ a constant. The form of equation (3) was suggested by Frederking *et al.* [10], to extend the applicability of Darcy's law into the

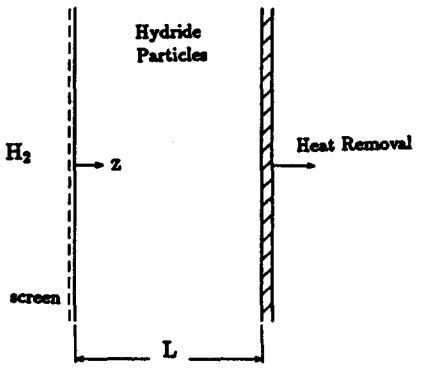

FIG. 1. The one-dimensional model hydride bed.

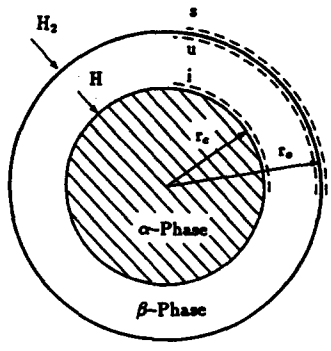

FIG. 2. The shrinking core model for a spherical hydride particle.

transitional flow regime. The constant ξ was determined to be 1.15 in the range $0.1 < Kn < 1$.

Thus

$$K_D = \frac{d_p^2 \varepsilon_b^3}{180(1-\varepsilon_b)^2}, \quad Kn = \lambda/L_c \tag{4}$$

with

$$L_c = K_D^{1/2}; \quad \lambda = \frac{\mu}{P}\left(\frac{\pi \mathscr{R} T}{2M}\right)^{1/2}. \tag{5}$$

Substituting equation (2) in equation (1) and assuming an ideal gas, gives

$$\frac{d}{dz}\left(\frac{K_{eff} M}{\mu \mathscr{R} T} P \frac{dP}{dz}\right) = \dot{r}(z,t). \tag{6}$$

Previous studies [11, 12] indicate that heterogeneous models may be more appropriate in cases of large exothermic reactions: the models use two energy equations, one for the solid and one for the gas. However, heat transfer in a fine powdered packed bed can be modeled assuming that the local gas and bed temperatures are equal, and ignoring storage in the gas phase [13]. The energy conservation equation is then

$$(1-\varepsilon_b)\rho_b c_b \frac{\partial T}{\partial t} = k_b \frac{\partial^2 T}{\partial z^2} - \rho_g u c_{pg} \frac{\partial T}{\partial z} + \dot{r}(z,t)\Delta H. \tag{7}$$

This heat transfer model is similar in principle to that used by Mayer *et al.* [9] except for the convection term, $\rho_g u c_{pg}(\partial T/\partial z)$. Results show that the influence of the convection term does not play a significant role when the inlet hydrogen temperature is the same as the bed temperature: it gives less than 1% difference in heat and mass transfer rate, and 3% difference in temperature distribution. However, in a heat pump system, the convection term is more significant since the hydrogen temperature can be much higher/lower than the bed temperature.

The kinetics of the hydriding process are described in terms of a shrinking core model: Fig. 2 shows such a model for an assumed spherical particle. The core is taken to be saturated α-phase metal, while hydride is the β-phase. The α-phase is a solid solution of hydrogen in the alloy lattice, and the β-phase is the stoichiometric hydride. Four steps are involved:

(i) chemisorption of H_2 molecules at the *s*-surface;
(ii) dissociation of the H_2 molecules into H atoms;
(iii) diffusion of H atoms through the hydride phase;
(iv) phase transformation at the hydride interface, $\alpha + H \rightarrow \beta$.

Accurate and reliable data are sparse for the hydrogen chemisorption process, and it is not known whether the second step is a general requirement for the absorption (or desorption) process [14]. There seems to be general agreement that the last two steps are probably the rate controlling steps, but there is considerable controversy as to the appropriate equations to describe these steps. For the diffusion step, Song and Lee [15] propose a shrinking core model. Then

$$\dot{m}_H = \frac{4\pi D(P_u^{1/2} - P_i^{1/2})}{1/r_c - 1/r_o} = 4\pi r_o D_0 \exp\left(-\frac{E_a}{\mathscr{R}T}\right)\frac{(P_u^{1/2} - P_i^{1/2})}{[(1-\omega)^{-1/3} - 1]} \tag{8}$$

which is the conventional result for constant property quasi-steady diffusion across a spherical shell. However Flanagan [14] suggests that, if the concentration dependence of the diffusion coefficient is allowed for, the driving force becomes $\ln(P_u/P_i)$. For the phase transformation step Song and Lee propose a linear driving force $(P_i - P_{eq})$ while Goodell and Rudman [16] use $\ln(P_i/P_{eq})$. Experimental data appears to favor the logarithmic driving forces, but the validity of the data is questionable owing to heat transfer and gas flow limitations. For the present work we have assumed the diffusion step to be rate limiting. The shrinking core model is used with an appropriate value of the diffusion coefficient determined from available experimental data. Then $\dot{r}(z,t)$ is obtained from equation (8) as

$$\dot{r}(z,t) = D^* \exp\left(-\frac{E_a}{\mathscr{R}T}\right)\frac{(P^{1/2} - P_{eq}^{1/2})}{[(1-\omega)^{-1/3} - 1]}; \quad D^* = 4\pi r_o D_0 n_0 \tag{9}$$

where P_u has been replaced by the local hydrogen pressure P, and P_i has been replaced by P_{eq}, the van't Hoff equilibrium pressure for saturated α-phase alloy. Nishizaki *et al.*'s modified equation is used for P_{eq} [17]

$$\ln P_{eq} = -\frac{A}{T} + B + (\phi \pm \phi_0)\tan[\pi(\omega - \tfrac{1}{2})] \pm \frac{\beta}{2} \tag{10}$$

where ϕ and ϕ_0 are plateau flatness factors and β the plateau hysteresis factor: a positive sign indicates absorption, and a negative sign, desorption.

With the source term specified it remains to give

initial and boundary conditions. For absorption the initial conditions are simply

$$t = 0: T = T_0, \quad P = P_{eq}(T_0) \tag{11}$$

while the boundary conditions are

$$z = 0: P = P_0, \quad -k_b \frac{\partial T}{\partial z} = \rho_s u c_{ps}(T_0 - T) \tag{12}$$

$$z = L: \frac{dP}{dz} = 0, \quad T = T_0. \tag{13}$$

The second boundary condition at $z = 0$ follows from the requirement of continuity of the energy flux at $z = 0$, while the second boundary condition at $z = L$ ignores the possibility of a contact resistance between the wall and the powder bed.

3. NUMERICAL SOLUTION PROCEDURE

The mathematical system comprises of a non-linear ordinary differential equation coupled to a linear partial differential equation. After some experimentation a non-linear shooting method was chosen for the o.d.e., and a finite difference method was chosen for the p.d.e. The major difficulty to be overcome was the solution of the o.d.e. at short times, for which pressure changes have not penetrated to the end of the bed at $z = L$. This regime lasts but a few seconds and its precise solution is of little consequence to the subsequent bed behavior. However it was found necessary to be careful with its solution in order to avoid a numerical divergence which can occur in the non-linear terms. The use of quasi-linearization and a finite difference scheme proved unsuitable; it was found that the non-linear shooting method allowed the problem to be traced and remedied. The p.d.e. was discretized in the Crank–Nicolson form, and the SOR method used for solving the resulting algebraic equations. Fixed point iterations through the two equations were conducted until the temperature distribution converged.

4. RESULTS AND DISCUSSION

The metal alloy chosen for this study was $LaNi_{4.9}Al_{0.3}$, since it is one of the few alloys for which reliable experimental data are available to establish the sorption kinetics. Supper *et al.* [8] measured hydrogen absorption rates in thin beds. A heat pipe was used to remove the heat of reaction, and it was found that isothermal conditions could be maintained provided the bed thickness did not exceed 2 mm. The required kinetics parameters in the shrinking core model, equation (8) were established as follows. First the apparent activation energy E_a, which is the activation energy for the diffusion of hydrogen atoms through the hydride phase, was set equal to 33.9 kJ $(\text{mol } H_2)^{-1}$ based on the work of Huston and Sandrock [18]. Then the parameter D^* was varied to obtain a best fit to the experimental data for a 2 mm thick bed at $T = 293$ K, with $P_0 = 3$ atm. The properties used for numerical calculations are tabulated in Table 1.

Figures 3(a)–(c) show the predicted hydrogen concentration ratio ω (defined as the amount of hydrogen absorbed/the maximum amount of hydrogen absorbed), and the dimensionless temperature θ (defined as $\theta = (T - T_0)/(T_{eq}(P_0) - T_0)$, where $T_{eq}(P_0)$ is van't Hoff's equilibrium temperature at P_0 and $\omega = 0.5$). The hydride particles have an initial hydrogen concentration of $\omega = 0.1$ and uniform temperature equal to the wall temperature, and there is a step change in the ambient hydrogen pressure to $P_0 = 3$ atm at $t = 0$. The curves indicate different locations in the hydride bed. Experimental data are shown for ω only since the bed was assumed to be isothermal by the experimenters. Furthermore, the measured values of ω were regarded to be some mean value in the bed, since measurement of ω profiles across such beds was impractical. A value of $D^* = 175$ was deemed to give a suitable match with experiment. The obvious discrepancy at small times could be due to a poor response of the pressure transducer or flow measuring device. Alternatively there could be a modeling error due to the neglect of the unsteady term in the flow equation, equation (1). Notice that, for these conditions, pressure drop is not the rate limiting factor.

Although Supper *et al.* [8] conducted their experiments at 2–5 atm pressure, a lower value is more appropriate for heat pump applications. Some essential features of bed behavior are shown in Figs. 4(a) and (b) which present local hydrogen concentration and temperature profiles as a function of time in a 10 mm thick bed for $T_0 = 293$ K, $P_0 = 1$ atm. The most striking feature is that absorption rates are faster closer to the cold wall. The reason for this behavior is seen in the temperature profiles, which show that, away from the cold wall, the bed temperature rises rapidly to a peak value of $\theta \sim 1.4$ and then decreases slowly. The relatively poor thermal conductivity of the hydride powder ($k \sim 1\ \text{W m}^{-1}\text{K}^{-1}$) requires large temperature gradients to conduct the heat of reaction to the cold wall, where it is transferred to the coolant. Since the equilibrium pressure P_{eq} is related to temperature by the van't Hoff equation, equation (10), an increased temperature increases P_{eq}, and hence decreases the driving force in equation (8). There is a competing effect near the wall where the lower temperatures decrease the absorption rate constant via the Arrhenius law temperature dependence of the diffusion coefficient in equation (8). Somewhat less important for this bed is the decrease in pressure across the bed required for the hydrogen flow, as will now be discussed.

Figures 5(a)–(c) show the pressure profiles for three bed thicknesses, namely 10, 20 and 30 mm. It is seen that, as the bed thickness increases above 10 mm there is a significant reduction in the pressure near the cold wall due to the resistance to hydrogen flow. The local

Table 1. $LaNi_{4.7}Al_{0.3}$ bed properties used for the numerical calculations

ε_b	void fraction	0.5	
ρ_b	density	2500.00	[kg m^{-3}]
c_α	heat capacity of α-phase	339.67	[J kg^{-1} K^{-1}]
c_β	heat capacity of β-phase	492.10	[J kg^{-1} K^{-1}]
d_p	average particle diameter	3.00	[mm]
k_b	thermal conductivity	1.3	[W m^{-1} K^{-1}]
$[H/M]_{max}$	hydrogen capacity	1.00	[mol$_H$ mol$^{-1}_{alloy}$]
A	constant in equation (10)	4068.00	
B	constant in equation (10)	12.92	
ϕ	plateau flatness factor	0.30	
ϕ_0	plateau flatness factor	0.005	
β	plateau hysteresis factor	0.098	

absorption rate decreases due to the reduced driving force in equation (8). The Knudsen number for these conditions is 0.94 indicating the transitional flow regime. According to equation (3) the effective permeability is more than twice the conventional Darcy permeability. We note that in the experiments of Supper *et al.* [8] the hydrogen pressure drop was not significant owing to the thin bed ($L = 2$ mm) and high pressure ($P = 3$ atm). Thus these data cannot be used to evaluate models for hydrogen flow.

The importance of the heat transfer limitation is clearly evident. Thus it is of interest to explore the effect of thermal conductivity. Several methods have been suggested for increasing the effective thermal conductivity of the bed, for example, addition of wire or metal powder of high thermal diffusivity, or use of an aluminum foam matrix to contain the hydride particles. Figure 6(a) shows the effect of effective thermal conductivity on hydrogen absorption rate: a value of $k_b = 1.3$ W m^{-1} K^{-1} corresponds to unenhanced alloy powder. It is useful to compare the absorption time constant since the rate of absorption

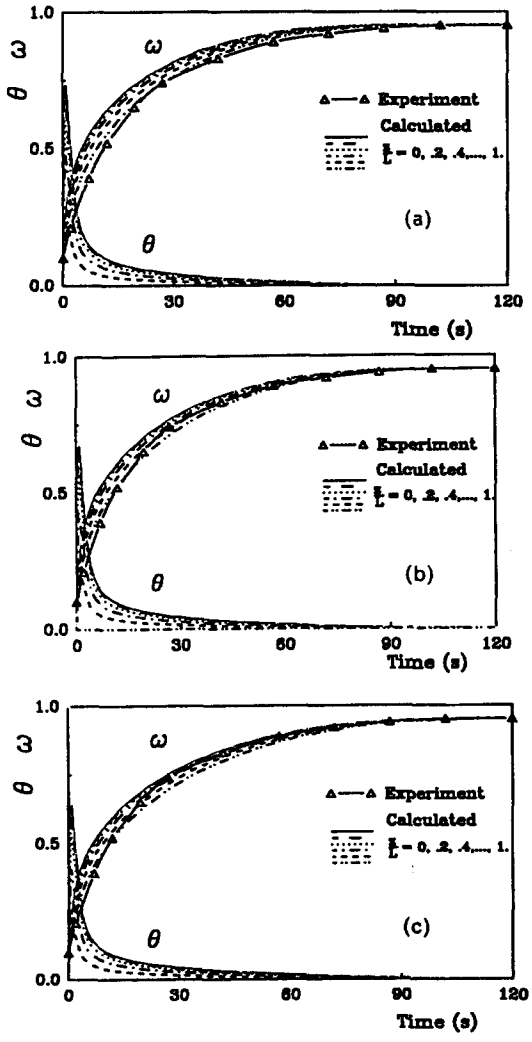

FIG. 3. Hydrogen concentration ratio and temperature profiles for the $LaNi_{4.9}Al_{0.3}$ bed of Supper *et al.* [8]. Comparison of theory with experiment for $L = 2$ mm, $P_0 = 3$ atm, $T_0 = 293$ K, and three values of D^*: (a) $D^* = 165$; (b) $D^* = 175$; (c) $D^* = 195$.

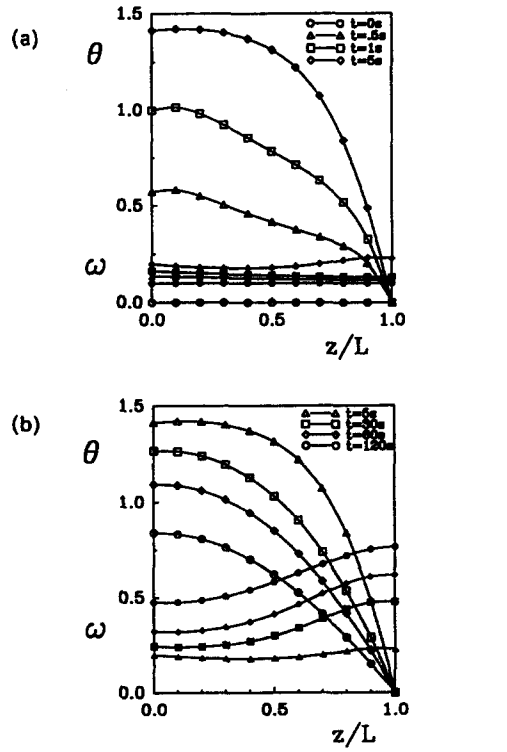

FIG. 4. Calculated hydrogen concentration ratio and temperature profiles for $L = 10$ mm, $P_0 = 1$ atm, and $T_0 = 293$ K: (a) $0 < t < 5$ s; (b) $5 < t < 120$ s.

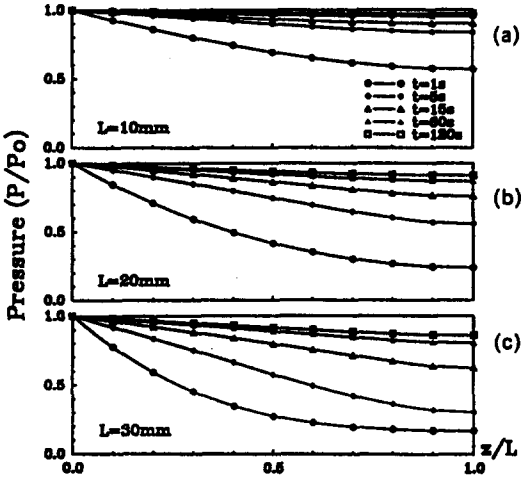

FIG. 5. Pressure profiles for $P_0 = 1$ atm, $T_0 = 293$ K, and three bed thicknesses: (a) 10 mm; (b) 20 mm; (c) 30 mm.

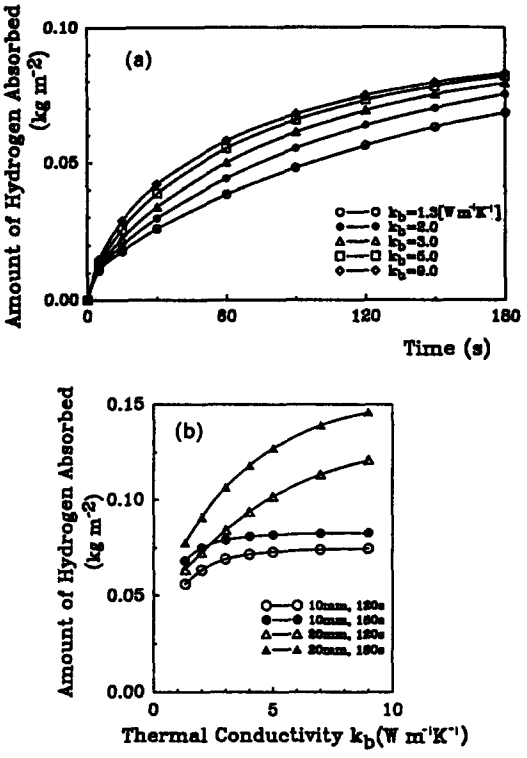

FIG. 6. Effect of bed effective thermal conductivity for $L = 10$ mm, $P_0 = 1$ atm, and $T_0 = 293$ K: (a) hydrogen absorption as a function of time; (b) hydrogen absorption as a function of effective thermal conductivity.

is the most important parameter controlling the mass of hydride required for a given heat load. Table 2 shows the time required to absorb hydrogen up to 80% as the effective thermal conductivity is increased.

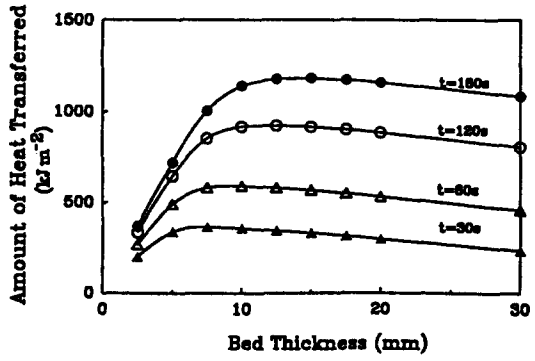

FIG. 7. Amount of heat transferred as a function of bed thickness, $P_0 = 1$ atm, $T_0 = 293$ K, $k_b = 1.3$ W m^{-1} K^{-1}.

The data in Fig. 6(a) are replotted in Fig. 6(b) vs effective thermal conductivity where it is seen that, for a reaction bed thickness of 10 mm, an increase up to a value of about 4 W m^{-1} K^{-1} gives a substantial improvement in the rate of hydrogen absorption, whereas an increase above a value of about 5 W m^{-1} K^{-1} yields little further improvement. This feature implies that, although heat transfer is the dominant limitation for unenhanced metal powder, if the effective thermal conductivity is increased above 5 W m^{-1} K^{-1}, hydrogen flow and reaction kinetics become the rate limiting processes. Furthermore, in space applications where system weight is a critical parameter, the effect of the added weight of the conductivity enhancement must be assessed. Figure 6(b) shows also that the heat transfer limitation is more significant in thicker beds.

Figure 7 shows the amount of heat transferred as a function of bed thickness, and is perhaps the most important result obtained in this study. It is seen that an optimum bed thickness exists: for example, the value is about 15 mm for a 3 min absorption time. In a thin bed the absorption rates are highest close to the cold wall and the conduction path for the heat of reaction is relatively short. As the bed thickness increases there is more alloy available for absorbing hydrogen, but the effect of pressure drop in the hydrogen flow causes not only the decrease of reaction driving force in equation (8), but also the location of the maximum absorption rate moves away from the cold wall towards the front of the bed, and the conduction path length increases. If the optimum thickness is exceeded, the gain due to having more hydride is negated by the increased conduction resistance for transfer of heat out of the bed. It must be noted, however, that the optimum bed thickness when weight considerations are included might differ from the value of about 10–15 mm established here. Figure 8

Table 2. Time to absorb 80% hydrogen; $L = 10$ mm, $P_0 = 1$ atm, and $T_0 = 293$ K

k_b	[W m^{-1} K^{-1}]	1.3	2.0	3.0	4.0	5.0	9.0
t	[s]	174.0	135.0	111.0	101.0	95.0	87.0

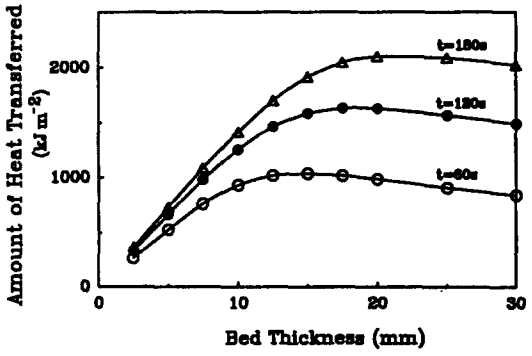

FIG. 8. Amount of heat transferred as a function of bed thickness, $P_0 = 1$ atm, $T_0 = 293$ K, $k_b = 5$ W m^{-1} K^{-1}.

shows similar results with enhanced thermal conductivity. The optimal bed thickness of an enhanced bed is larger than that of an unenhanced bed. Taking just the hydride weight into account the optimum thickness will be less, but, when the weight of the heat exchanger surface and coolant plumbing is included, a larger value may result.

5. CONCLUSIONS

(1) A satisfactory model of a metal hydride bed must account for heat conduction, hydrogen flow, and sorption kinetics.

(2) Available experimental data can be used to establish the model parameters for $LaNi_{4.7}Al_{0.3}$ alloy.

(3) For $LaNi_{4.7}Al_{0.3}$ alloy the following observations can be made:

(i) for beds less than about 5 mm thick and pressures greater than about 2 atm, pressure drop due to hydrogen flow is not a rate limiting factor;

(ii) augmentation of thermal conductivity up to about 4 W m^{-1} K^{-1}, leads to significant improvement of performance for bed thickness of about 10 mm;

(iii) optimum bed thicknesses for heat pump application are in the range 10–15 mm for an unenhanced bed.

Acknowledgements—This work was supported by the San Jose State University Foundation on subcontract 057-6. The Principal Investigator was Dr D. K. Edwards, Department of Mechanical Engineering, University of California, Irvine. Computer time was supplied by the Campus Computing Network of the University of California, Los Angeles.

REFERENCES

1. H. I. Abelson and J. S. Horowitz, Thermodynamic analysis of a metal–hydride heat pump, *J. Energy* **5**(4), 237–243 (1981).
2. S. Suda, Metal hydrides, *Int. J. Hydrogen Energy* **12**(5), 323–331 (1987).
3. J. A. Jones and P. M. Golben, Design life testing, and future designs of cryogenic hydride refrigeration systems, *Cryogenics* **25**, 212–219 (April 1985).
4. J. I. Rodriguez and A. F. Mills, Development of a solid hydrogen sorption stage, JPLD-5070, Phase I, Final Report, February (1988).
5. O. Bernauer, Metal hydride technology, *Int. J. Hydrogen Energy* **13**(3), 181–190 (1988).
6. A. Yanoma, M. Yoneta, T. Nitta and T. Okuda, Design and operation of the commercial size chemical heat pump system using metal hydrides, *Proc. ASME–JSME Thermal Engng Joint Conf.*, Vol. 5, pp. 431–437 (1987).
7. P. Dantzer and E. Orgaz, Thermodynamics of hydride chemical heat pump—II. How to select a pair of alloys, *Int. J. Hydrogen Energy* **11**(12), 797–806 (1986).
8. W. Supper, M. Groll and U. Mayer, Reaction kinetics in metal hydride reaction beds with improved heat and mass transfer, *J. Less-Common Metals* **104**, 279–286 (1984).
9. U. Mayer, M. Groll and W. Supper, Heat and mass transfer in metal hydride reaction beds: experimental and theoretical results, *J. Less-Common Metals* **131**, 235–244 (1987).
10. T. H. K. Frederking, W. A. Hepler and P. K. Khandhar, Slip effects associated with Knudsen transport phenomena in porous media, *Space Cryog. Workshop*, Madison, Wisconsin, Paper B-5 (1987).
11. M. Riaz, Transient analysis of packed-bed thermal storage system, *Solar Energy* **21**, 123–128 (1978).
12. S. I. Pereira Duarte, O. A. Ferretti and N. O. Lemcoff, A heterogeneous one-dimensional model for non-adiabatic fixed bed catalytic reactors, *Chem. Engng Sci.* **39**(6), 1025–1031 (1984).
13. H. Choi, Hydride heat pumps for upgrading spacecraft waste heat, Ph.D. Dissertation, School of Engineering and Applied Science, University of California, Los Angeles (1989).
14. T. B. Flanagan, Kinetics of hydrogen absorption and desorption, *Hydrides for Energy Storage: Proc. Int. Symp.*, Geilo, Norway, 14–15 August, pp. 135–150 (1977).
15. M. Y. Song and J. Y. Lee, A study of the hydriding kinetics of Mg–(10–20 w/o) $LaNi_5$, *Int. J. Hydrogen Energy* **8**(5), 363–367 (1983).
16. P. D. Goodell and P. S. Rudman, Hydriding and dehydriding rates of the $LaNi_5$–H system, *J. Less-Common Metals* **89**, 117–125 (1983).
17. T. Nishizaki, K. Miyamoto and K. Yoshida, Coefficients of performance of hydride heat pumps, *J. Less-Common Metals* **89**, 559–566 (1983).
18. E. L. Huston and G. D. Sandrock, Engineering properties of metal hydrides, *J. Less-Common Metals* **74**, 435–443 (1980).

TRANSFERT DE CHALEUR ET DE MASSE DANS DES LITS D'HYDRURE METALLIQUE POUR DES APPLICATIONS DE POMPE A CHALEUR

Résumé—On modélise le transfert de chaleur et de masse dans un lit d'hydrure métallique. Le modèle inclut la conduction thermique, l'écoulement d'hydrogène selon la loi de Darcy modifiée pour le régime de transition et la cinétique de sorption qui suppose que la diffusion à travers l'hydrure est limitante. Les paramètres du modèle correspondent à l'alliage $LaNi_{4.7}Al_{0.3}$ en utilisant des données expérimentales. Des calculs paramétriques pour une application de la pompe à chaleur à un véhicule spatial montrent les effets du transfert de chaleur, de l'écoulement d'hydrogène et les limitations de la cinétique de sorption. On montre l'effet de l'accroissement de la conduction thermique. Les épaisseurs optimales du lit sont dans la plage 10–20 mm pour un temps d'absorption de 3 min et $k_b = 1{,}3 \sim 5$ W m^{-1} K^{-1}.

WÄRME- UND STOFFTRANSPORT IN METALLHYDRIDBETTEN FÜR WÄRMEPUMPENANWENDUNGEN

Zusammenfassung—Der Wärme- und Stofftransport in einem Metallhydridbett wird modelliert. Das Modell enthält Wärmeleitung, die Strömung von Wasserstoff (gemäß dem Darcy'schen Gesetz, das für das Übergangsgebiet der Strömung modifiziert wird) und die Sorptionskinetik (unter der Annahme, daß die Diffusion im Hydrid für das Problem limitierend wirkt). Die Modellparameter werden unter Verwendung von Versuchsdaten für $LaNi_{4.7}Al_{0.3}$ eingestellt. Die Parametervariationen für eine Wärmepumpenanwendung in einem Raumfahrzeug zeigen die konkurrierenden Effekte von Wärmetransport, Wasserstoffströmung und Sorptionskinetik. Die günstige Wirkung einer verbesserten Wärmeleitung wird aufgezeigt. Die optimale Dicke des Reaktionsbettes scheint im Bereich 10 bis 20 mm für eine Absorptionszeit von 3 Minuten und $k_b = 1{,}3 \sim 5\ W\ m^{-1}\ K^{-1}$ zu liegen.

ТПЛО- И МАССОПЕРЕНОС В СЛОЯХ ГИДРИДОВ МЕТАЛЛОВ ПРИМЕНИТЕЛЬНО К ТЕПЛОВЫМ НАСОСАМ

Аннотация—Моделируется тепло- и массоперенос в слое гидрида металла. Модель включает теплоперенос, течение водорода, определяемое модифицированным для неустановившегося режима течения законом Дарси, а также кинетику сорбции в предположении, что диффузия через гидряд является стадией, определяющей скорость процесса. На основе имеющихся экспериментальных данных найдены параметры модели для сплава $LaNi_{4.7}Al_{0.3}$. Расчеты параметров для тепловых насосов применительно к космическим аппаратам выявляют ограничения, связанные с конкурирующими эффектами: теплопереносом, течением водорода и процессами сорбции. Иллюстрируется эффект увеличения теплопроводности. Найдено, что толщина слоя оптимальна в диапазоне 10–20 мм в течение 3 минут времени сорбции при $k_b = 1{,}3 \sim 5\ W\ m^{-1}\ K^{-1}$.